

## A model for the improvement of thermal bridges quantitative assessment by infrared thermography



Giorgio Baldinelli<sup>a,\*</sup>, Francesco Bianchi<sup>a</sup>, Antonella Rotili<sup>a</sup>, Danilo Costarelli<sup>b</sup>, Marco Seracini<sup>b</sup>, Gianluca Vinti<sup>b</sup>, Francesco Asdrubali<sup>c</sup>, Luca Evangelisti<sup>c,d</sup>

<sup>a</sup> Department of Engineering, University of Perugia, Via G. Duranti, 67, 06125 Perugia, Italy

<sup>b</sup> Department of Mathematics and Computer Science, University of Perugia, Via Vanvitelli, 1, 06123 Perugia, Italy

<sup>c</sup> Department of Engineering, University of Roma Tre, Via V. Volterra, 62, 00146 Rome, Italy

<sup>d</sup> Department of Engineering, Niccolò Cusano University, Via don Carlo Gnocchi 3, 00166 Rome, Italy

### HIGHLIGHTS

- Improvement of energy diagnosis of the building envelope.
- Influence factor of the thermal bridge definition and improvement.
- Experimental campaign in the Hot Box apparatus performing thermal analysis on thermal bridges sample.
- Mathematical algorithm for the enhancement of the image resolution.
- Physical contours extracting method of thermal bridges from the infrared image.

### ARTICLE INFO

#### Keywords:

Thermal bridges  
Energy building diagnosis  
Quantitative infrared thermography  
Image enhancement  
Hot box

### ABSTRACT

The intervention on the existing building envelope thermal insulation is the main and effective solution in order to achieve a significant reduction of the building stock energy needs. The infrared technique is the methodology of the energy diagnosis aimed to identify qualitatively the principal causes of energy losses: the presence of thermal bridges. Those weak parts of the building envelope in terms of heat transfer result not easy to treat with an energy efficiency intervention, while they are gaining importance in the buildings total energy dispersion, as the level of insulation of opaque and transparent materials is continuously increasing. It is generally possible to evaluate the energy dispersions through these zones with a deep knowledge of the materials and the geometry using a numerical method. Besides, authors proposed in the past a methodology to assess the flux passing through thermal bridges with an infrared image correctly framed. The analysis of surface temperatures of the undisturbed wall and of the zone with thermal bridge, allows to define the *Incidence Factor of the thermal Bridge* ( $I_{tb}$ ). This parameter is strongly affected by the thermographic image accuracy, therefore, this paper deals with the development and validation of an innovative mathematical algorithm to enhance the image resolution and the consequent accuracy of the energy losses assessment. An experimental campaign in a controlled environment (hot box apparatus) has been conducted on three typologies of thermal bridge, firstly performing the thermographic survey and then applying the enhancement algorithm to the infrared images in order to compare the  $I_{tb}$  and the linear thermal transmittance  $\psi$  values. Results showed that the proposed methodology could bring to an accuracy improvement up to 2% of the total buildings envelope energy losses evaluated by quantitative infrared thermography. Moreover, the proposed algorithm allows the implementation of a further process applicable to the images, in order to extract the physical boundaries of the hidden materials causing the thermal bridge, so revealing itself as a useful tool to identify exactly the suitable points of intervention for the thermal bridge correction. The application of the imaging process on the quantitative infrared thermography is an innovative approach that makes more accurate the evaluation of the actual heat loss of highly insulating buildings and reaching a higher detail on the detection and treating of thermal bridges.

\* Corresponding author.

E-mail address: [giorgio.baldinelli@unipg.it](mailto:giorgio.baldinelli@unipg.it) (G. Baldinelli).

**Nomenclature**

$A$	area (m <sup>2</sup> )
$I$	incidence factor (–)
$l$	length (m)
$N$	number of pixels
$R$	scaling factor
$Q$	heat flux (W)
$T$	temperature (K)
$TB1$	thermal bridge sample 1
$TB2$	thermal bridge sample 2
$TB3$	thermal bridge sample 3
$P$	peak
$U$	thermal transmittance (W/m <sup>2</sup> K)

$\varphi$	density of thermal flux (W/m <sup>2</sup> )
$\psi$	linear thermal transmittance (W/m K)

**Subscripts**

$i$	internal air
$p$	relative to each pixel
$1D$	one-dimensional
$HFM$	evaluated with heat flux meter
$tb$	thermal bridge
$tb_k$	relative to $k$ th heat flux meter
$1$	relative to peak 1
$2$	relative to peak 2
$m$	relative to the minimum between two peaks

**1. Introduction**

Most of the European building stock is made of existing constructions and the improvement of the envelope insulation (together with old thermal plants replacement) constitutes the primary intervention to reduce the energy consumption of the building sector [1]. The experimental analyses of the opaque and transparent elements insulation performance complements the theoretical approach, at the aim of reaching the assessment of the real building energy needs [2,3].

The thermographic survey on the building envelope is a useful method to detect defects and irregularities responsible of the reduction of its overall energy performance. According to the depth and scope of the audit, different evaluations may arise from the analysis of the thermographic images. A first approach can give qualitative information of the proper placement of the building element, eventually suggesting possible solutions. A deeper reading of the thermogram, with an accurate definition of the measurement conditions, leads to a quantitative analysis that supplies data about the heat transfer on the studied element [4]. For the retrofit process of a building envelope it results strategic to lead a deep energy diagnosis on the real conditions of the overall elements of the building [5,6]. The quantitative thermography helps designers and manufacturers to improve the current energy behavior of the building envelope, in particular zones such as thermal bridges, which play a more and more important role in the global energy dispersion of buildings.

Grinzato et al. [7] studied the application of the infrared thermography to detect defects in civil constructions. Air leakages, moisture problems, plaster detachments and thermal bridges in buildings can be detected using thermographic inspections. The authors consider that the quantitative methodology is a helpful technique to solve inverse heat conduction problems in transient regime.

Zalewski et al. [8] analysed thermal bridges in a light wall with a

steel frame, aiming to realise a support for designers. The thermal bridges were detected by means of infrared thermography, then the heat flow and surface temperatures were measured. A numerical simulation was carried out to predict the heat losses and this model was validated by the measured parameters.

When the building envelope is investigated with infrared thermography, a correct interpretation of the images is needed to identify the real defects. In fact, several parameters can affect the retrieved surface temperature, such as environmental conditions, emissivity and reflected temperature [9–11].

Lehmann et al. [12] tried to reduce misunderstandings in the interpretation of the thermal images, carrying out a numerical study on the environmental conditions to better understand the effects on the thermograms.

Building diagnoses were usually carried out by means of a passive approach and images were interpreted by qualitative or quantitative methods. Fokaides and Kalogirou [13] proposed a methodology to calculate the thermal transmittance of a building element through the retrieval of its external surface temperature by infrared cameras. The thermal transmittance was calculated from the heat transferred to the camera by radiation and convection. They analysed five dwellings during winter and summer season, comparing the standard transmittances with those evaluated by the infrared images and those estimated by thermohygroscopic measurements. They found that the values calculated with the measured temperature differ from 10% to 20% in terms of absolute deviation with respect to the ones estimated with theoretical input. They also noted that the measured temperature was particularly affected by the variation of emissivity and reflected temperature.

Albatici et al. [14] presented a measurement procedure and its validation: five different walls of an experimental building were analysed during three winter seasons from 2010 to 2013. The thermal

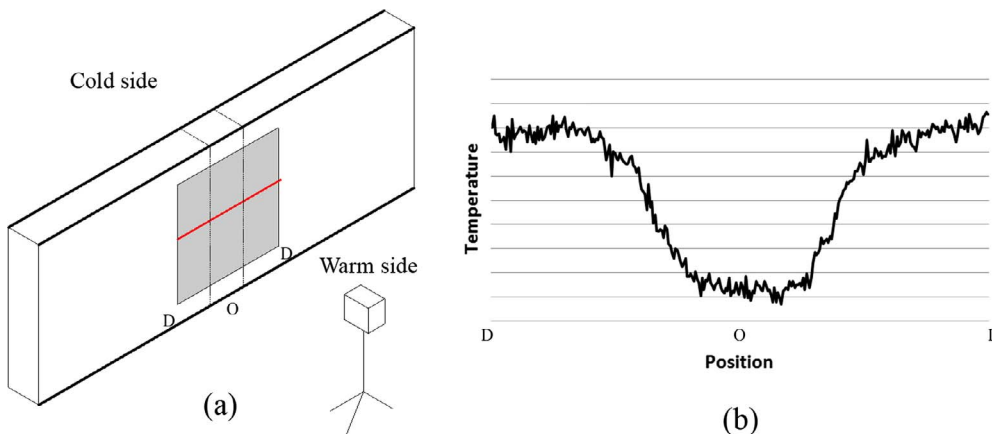


**Fig. 1.** Sketch of the structural pillar thermal bridge (a) and IR thermography temperature trend (b) in the red line. (For interpretation of the references to color in this figure legend, the reader is referred to the web version of this article.)

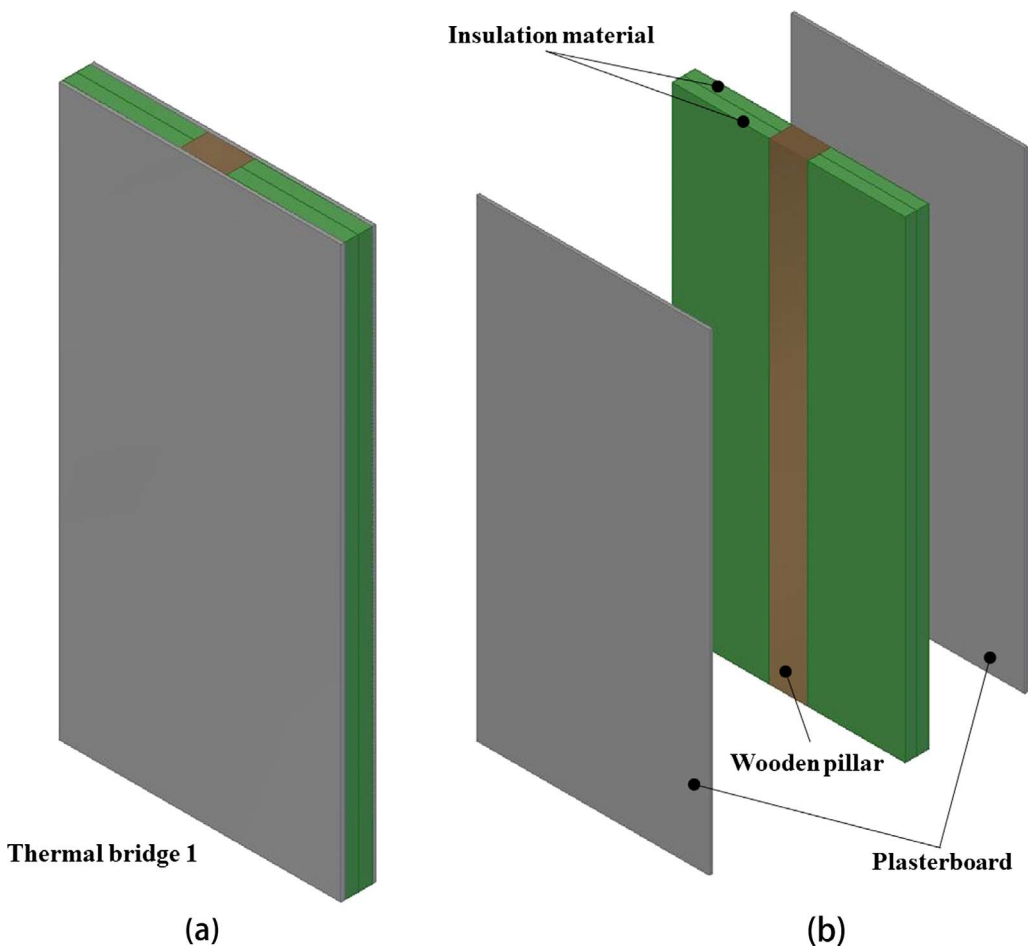


Fig. 2. Virtual model of thermal bridge n.1 (a) and exploded view with materials (b).

transmittance was calculated from parameters measured by thermographic surveys and on-site results were compared with design values. As far as heavy walls they found a high repeatability index and they also evidenced the influence of environmental conditions on the reliability of the results. The parameters with the highest impact on the outcomes resulted the surface and external environmental temperatures; walls exposure also affected the measurements accuracy.

Ohlsson and Olofsson [15] investigated the systematic error in the evaluation of the heat flow density from thermographic measurements, observing that the results of the thermographic approach were affected by the chosen heat convection coefficient model.

A laboratory study was performed by O'Grady et al. [16] in order to analyse the linear thermal transmittance value  $\psi$  as a function of the external wind influence. A thermal bridge set-up was built in a hot box apparatus and several tests were performed with different air velocities. The authors found a strong influence of  $\psi$  with the wind velocity and they proposed a methodology for the standardization of this value.

Asdrubali et al. [17] defined an index (the *Incidence factor of the thermal bridge*) for the quantitative evaluation of the heat losses due to the thermal bridge on the buildings envelope; the present paper is aimed at improving the methodology proposed using an enhancement of the thermographic image with a mathematical algorithm. In particular, the algorithm for the image reconstruction and enhancement based on the mathematical theory of the sampling Kantorovich operators has been applied [18–21], together with a suitable thresholding method, based on the histograms analysis associated to the thermographic image. The image reconstruction algorithms reveal useful to better define the temperature trend retrieved from infrared cameras, which are usually characterised by a mediocre pixel resolution. The image enhancement is aimed to improve the accuracy of the

methodology results, which depends significantly from the quality of the thermograms. Therefore, an improvement on the evaluation of the *Incidence factor of the thermal bridge* leads to a more accurate procedure of the energy diagnosis of the real conditions of the building envelope, with particular focus on the quantitative definition of thermal bridges.

The aforementioned improvement of the *Incidence factor of the thermal bridge* ( $I_{tb}$ ) has been obtained by means of a set of thermal bridges investigated in a hot box apparatus with controlled laboratory conditions. In addition, the procedure proposed in the present work allows to detect the geometrical shape of the thermal bridge, an information particularly useful for its thermal correction.

## 2. Methodology

An infrared camera is able to measure the energy emitted by objects in the infrared radiation field, in order to calculate their surface temperature.

A building opaque wall is composed by several materials able to transfer heat in different ways according to their thermophysical properties. Even if the internal wall is invisible to the human eyes, the infrared camera is able to detect the consequence of different thermal conductivities of materials. For instance, Fig. 1(a) shows a wall with a structural pillar inside. The gray zone is the framing of the infrared camera from the internal side of the building. In winter season the wall is subjected to a temperature difference between the indoor and outdoor environment. The detector of the infrared camera can “see” the temperature surface of the internal wall, that is U-shaped, as shown in Fig. 1(b), because of the presence of the pillar that generally is not or less insulated respect to the other zones of the wall.

The depth of the U-shape is strongly linked to the thermal bridge

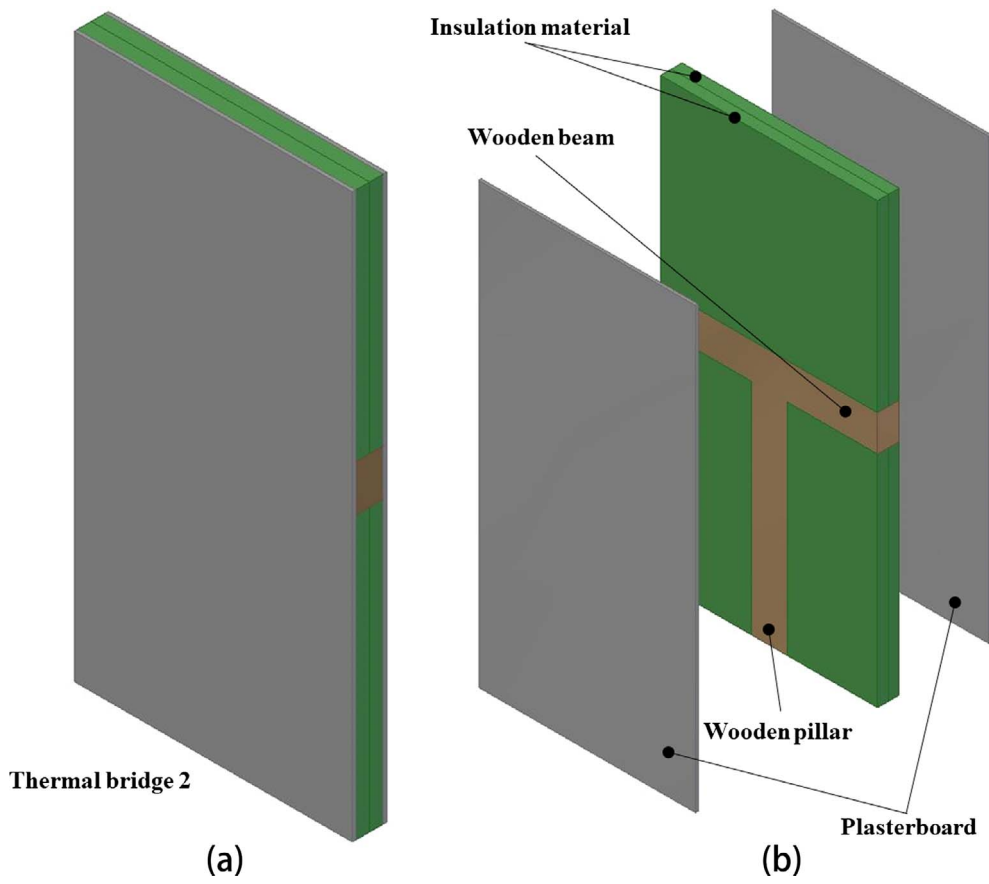


Fig. 3. Virtual model of thermal bridge n.2 (a) and exploded view with materials (b).

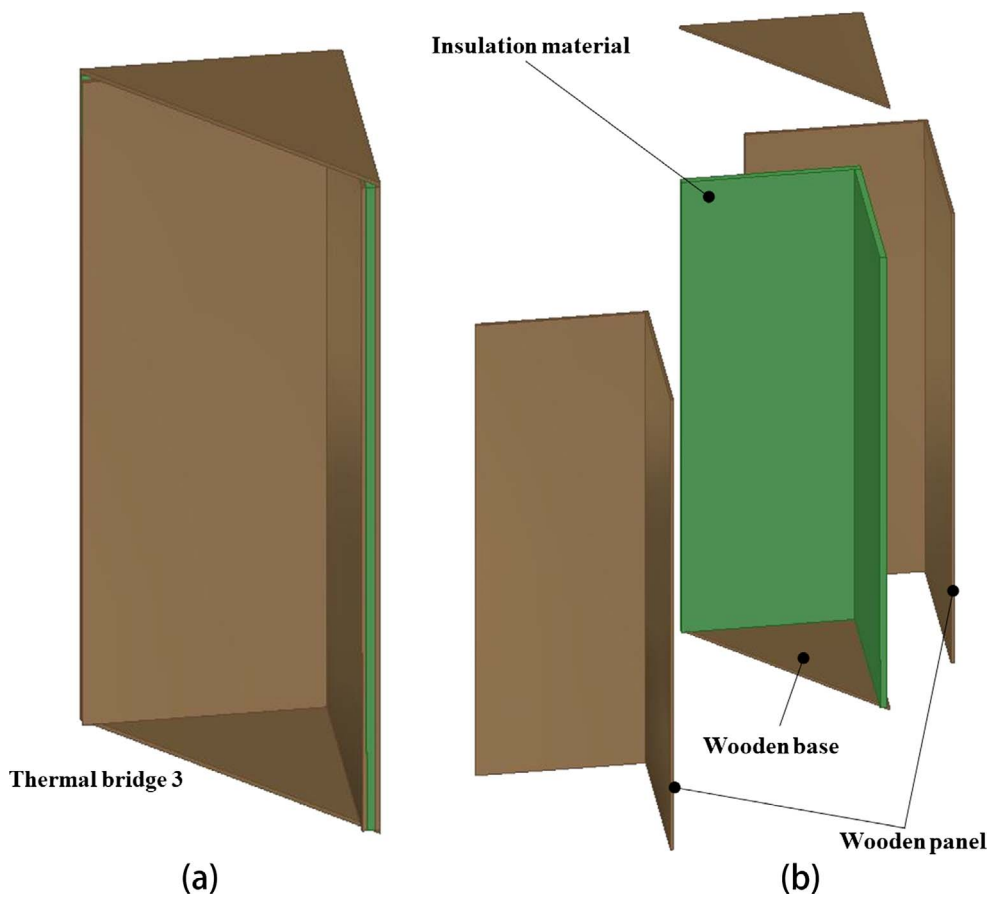


Fig. 4. Virtual model of thermal bridge n.3 (a) and exploded view with materials (b).

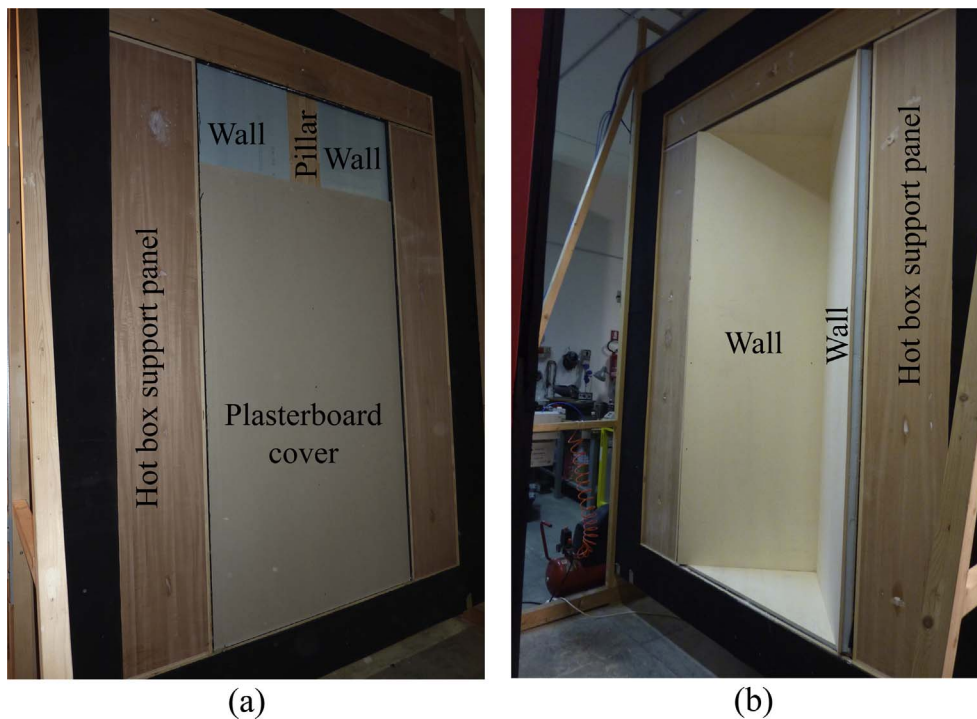


Fig. 5. Examples of the samples tested in the hot box: (a) structural pillar – TB1 and (b) corner between two walls – TB3.

weakness. The definition of  $I_{tb}$  is following reported [17]:

$$I_{tb} = \frac{\sum_{p=1}^N (T_i - T_p)}{N(T_i - T_{1D})} \quad (1)$$

where  $T_i$  is the internal air temperature,  $T_p$  is the acquired surface temperature of the single pixel from the infrared camera,  $T_{1D}$  is the surface temperature of the undisturbed zone of the wall, evaluated with the infrared camera as well, and  $N$  is the number of the pixels that compose the imaginary line along the thermal bridge.  $I_{tb}$  is a number higher than 1 and gives information on the thermal bridge effects on the overall energy performance of the investigated wall.

### 3. Measurements set-up

The thermal bridges were built and installed in a calibrated hot box apparatus [22]. The samples have been inserted in a central support dividing two conditioned chambers, called “hot” and “cold” room. The heat flow, in steady-state conditions, was obtained maintaining a constant temperature difference between the two chambers.

Three cases of thermal bridge were recreated:

- (1) 2D thermal bridge – pillar;
- (2) 2D thermal bridge – beam/pillar joint;
- (3) 2D thermal bridge – wall/wall joint.

The thermal bridge n.1 (TB1) was created by a timber beam, with dimensions 120 mm × 200 mm × 2450 mm, vertically stood in the central support, with both sides covered with a 15-mm-thick plasterboard panel. 60 mm thick polystyrene panels were used as insulator, positioned between the two layers of plasterboard (Fig. 2).

The same technique was applied to build the thermal bridge n.2 (TB2), except for the two timber beams arranged to form a T-shaped cross section, which was 1.35 m high and 1.21 m long (Fig. 3).

The thermal bridge n.3 (TB3), which had upper and lower triangular basis, was realized with plywood panels 15 mm thick, insulated with polystyrene panels of 30 mm thick. The base and the ceiling were realized with plywood as well. Each specimen covers a surface of 1.21 m × 2.45 m (Fig. 4), and it was inserted in the central frame

(support panel) between the two chambers.

Fig. 5 shows the structures TB1, and TB3 built inside the hot box setup (TB2 is quite similar to TB1).

The thermal images were obtained by means of an infrared thermal camera, with a resolution of 320 × 240 pixel and a spectral range of 7–13 μm (FLIR model B360).

Before the investigation start, the main parameters influencing the quality of an infrared quantitative measurement have been evaluated. In particular, the emissivity and reflectivity of the object may affect the calculation of the surface temperature [23].

The thermal camera was positioned on a tripod in the hot room, with a distance of 1.3 m from the object, in order to visualize both the thermal bridge and the undisturbed zones.

The environmental conditions were monitored during the experiment by probes: air temperature and relative humidity have been acquired and used in the infrared thermal image post-processing phase.

The surface emissivity of specimen was measured by D&S Emissometer, Model AE1, and the reflected temperature was determined by the reflector method, using a crumbled aluminum foil [24] positioned upon the specimen and visualized by the camera, setting the emissivity equal to 1. The average temperature retrieved by the camera was assumed to be the reflected temperature of the sample.

### 4. Heat flow and temperature measurements

The thermographic analysis is affected by numerous uncertainties and as the goal of the paper consists of focusing on the mathematical improvement of the *Incidence factor of the thermal bridge*, direct heat flux and temperature measurements were performed during the infrared camera surveys, in order to compare the thermographic outcomes and their improvement with sensor measurements.

A group of temperature and heat flow probes have been placed in the investigation area. The heat flow meters allow the measurement of the heat flux density ( $W/m^2$ ) in the undisturbed zone and throughout the whole area of the thermal bridge.

In order to calculate the *Incidence factor of the thermal bridge* using the sensors method, the surface temperatures were measured by thermocouples and the heat flow was retrieved by heat flow meters.

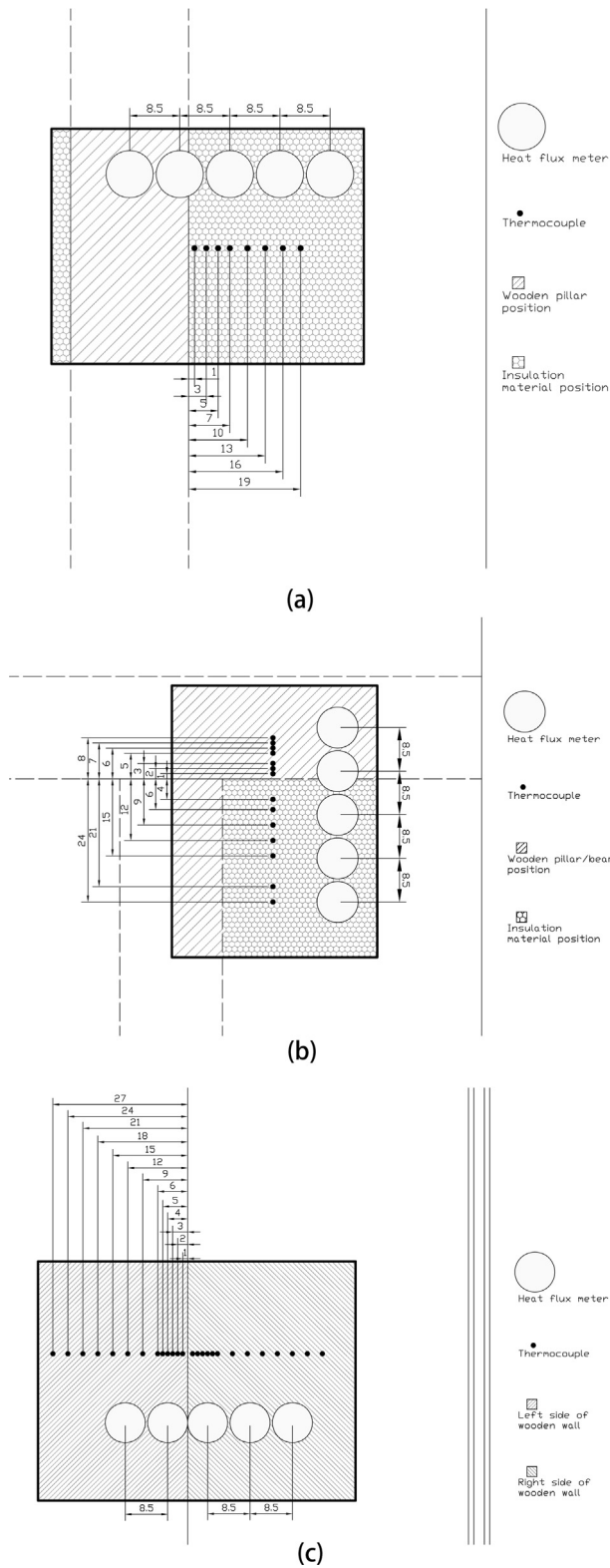


Fig. 6. Position [cm] of the probes on (a) the TB1 surface, (b) the TB2 surface and on (c) the TB3 surface; the thermographic framing is defined by the thick rectangle.

The temperature data were useful to minimize the thermographic error, matching the surface probes values with thermographic data and by means of the Ordinary Least Squares theory.

The Incidence factor of the thermal bridge is estimated with the probes using following equation [17]:

$$I_{tbHFM} = \frac{Q_{tb}}{Q_{1D}} = \frac{\varphi_{1D}A_{1D} + \sum_{k=1}^{n-1} \varphi_{tbk}A_{tbk}}{\varphi_{1D}(A_{1D} + \sum_{k=1}^{n-1} A_{tbk})} \quad (2)$$

where  $\varphi$  is the heat flux density retrieved by each heat flow meter and  $A$  is its pertinent area. The subscripts define the position of heat flow meter:  $tb_k$  indicates the probes placed in the influence zone of the thermal bridge, 1D indicates the heat flow meter placed in the undisturbed zone. Although the thermographic technique gives fields of temperature, the calculation of  $I_{tb}$  is basically a ratio between heat fluxes [17]; therefore, it can be assumed that the results of Eq. (2) is accurately representative of the heat flows through the wall.

The heat flow meters and the temperature probes were placed in the domain indicated by the proposed method [17], numerous thermocouples and heat flow meters were arranged along the lines to calculate the elements of Eq. (2). Fig. 6 shows the position of the probes for each thermal bridge along the domain and the framing of the thermal camera (thick rectangle). The three domains are following described:

- (a) a horizontal line, connecting the middle of the beam to the lateral panel, was chosen for TB1;
- (b) a vertical line represented the linear domain of the TB2. Moreover, at the aim of combining the effect of pillar and beam, an area has been used to define the areal domain;
- (c) a horizontal line was chosen for the TB3.

Finally, the thermography analysis and the probes data acquisition in the hot box apparatus were carried out simultaneously.

The accuracy of the two methods is characterized by the uncertainty values of the instrumentation. Generally speaking, the thermography technique results are affected by numerous variables: the controlled environment, the measurement of emissivity and reflected temperature and the correction linked to the contact temperature probes make the error equal to the value reported in the data sheet of the infrared camera: the 2% of the reading value [24]. The thermal flux measurements are characterised by an error equal to 5% of the reading value, as reported in the data sheet of the heat flux meters manufacturer [25].

### 5. Mathematical enhancement of the thermal bridges assessment: Procedure and validation

The Incidence factor of the thermal bridge has been calculated for each specimen installed in the hot box apparatus. Fig. 7(a) shows the analysed infrared image in the domain of interest and in Fig. 7(b) the surface temperatures acquired from both the infrared camera (green dotted line) and the temperature probes (red squares) for the thermal bridge TB1 are sketched. The 0 position on the x-axis is the point where the black horizontal line (x-domain) encounters the separation line between the pillar and the undisturbed zone. As stated above, the thermographic data have been fitted (Ordinary Least Squares method) with the probe temperatures to minimize the thermographic error. Fig. 7(b) shows also the temperature trend after the correction (blue<sup>1</sup> line).

According to Eqs. (1) and (2), the Incidence factor of the thermal bridge was calculated for both methodologies (infrared camera and heat flux probes): the values present a deviation close to 11%.

Fig. 8(a) shows the thermal bridge TB2. The domain ( $I_{tb2}$ ) is a line that has been analysed in Fig. 8(b) with the temperature probes and the heat flow meters as well. In this case, the position is represented in the y-axis. The results of this analysis show a deviation of around 11%, a value similar to the previous test.

The thermal bridge TB3 presents a different nature as it has a geometrical origin. In the TB1 and TB2 the singularities were created by

<sup>1</sup> For interpretation of color in Fig. 7, the reader is referred to the web version of this article.

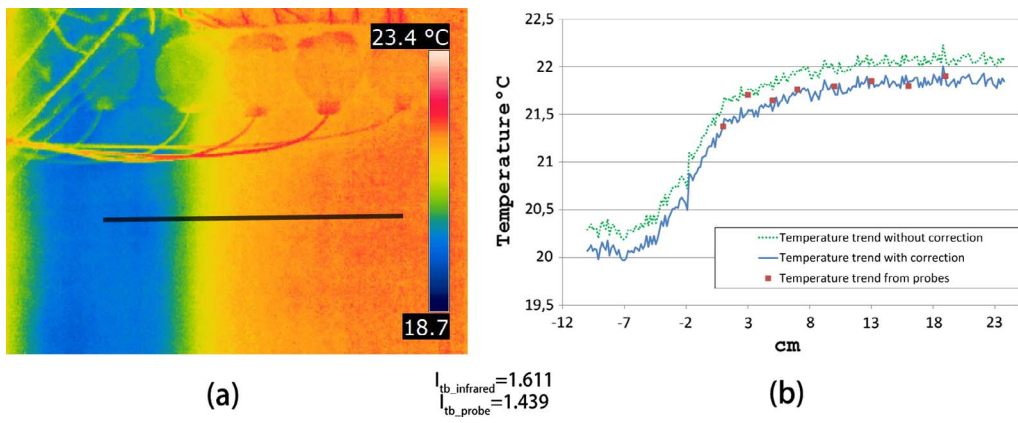


Fig. 7. Pillar thermal bridge (TB1): thermogram (a) and temperature trends (b).

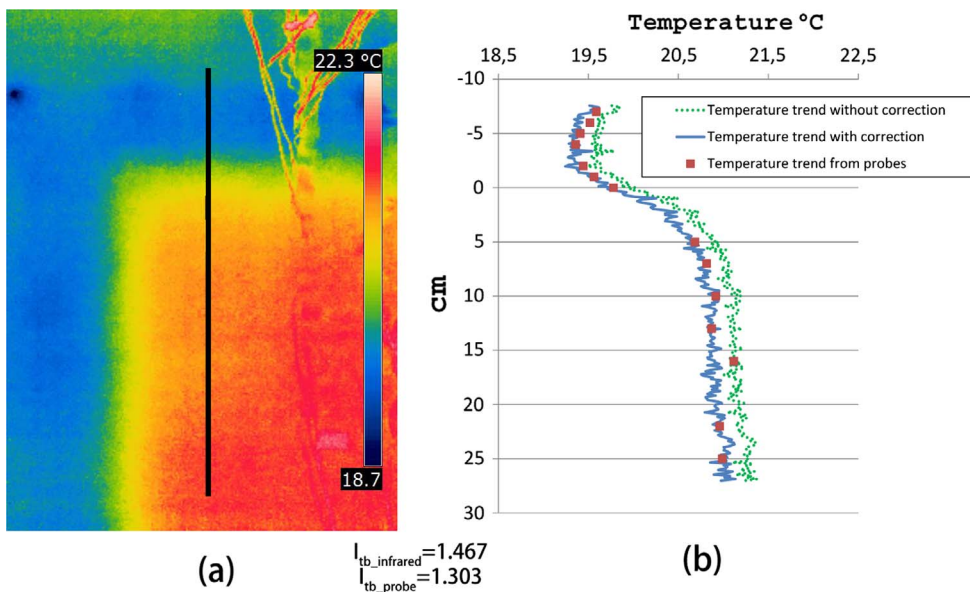


Fig. 8. Beam corner thermal bridge (TB2): thermogram (a) and temperature trends (b).

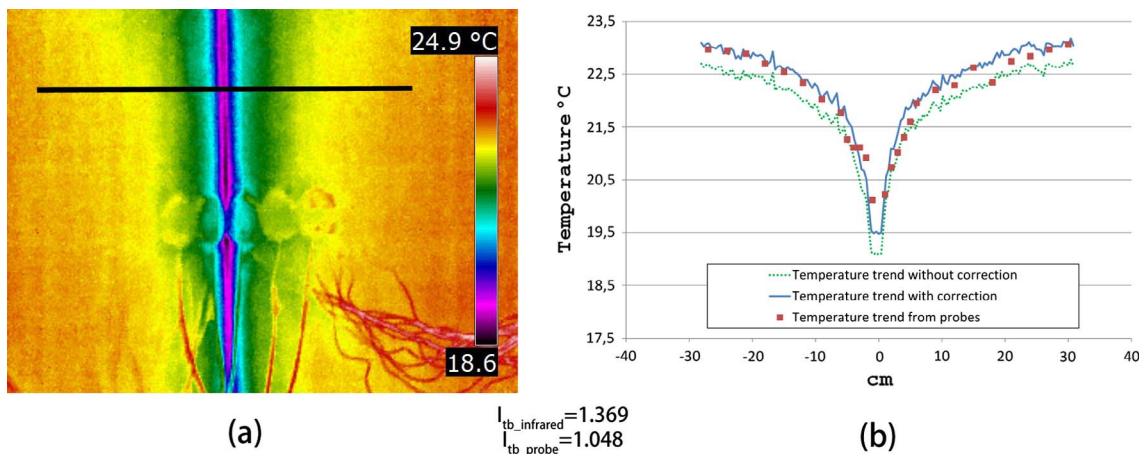


Fig. 9. Corner thermal bridge (TB3): thermogram (a) and temperature trends (b).

different material inside the wall, while for TB3 the thermal bridge is caused by the corner shape (Fig. 9). In this case, the two values of  $I_{tb}$  show a larger deviation respect to TB2, and TB3, with a result of around 23% difference between the thermographic methodology and probes analysis. This last result is probably due to the difficulty of placing the heat flow meter very close to the corner. The heat flow meters used have a diameter of 80 mm, including the guard zone. Thus, the sensible

element starts around 20 mm from the corner as shown in Fig. 9(a), losing the first part of V-shaped trend that strongly affects the thermal bridge effect.

From the *Incidence factor of the thermal bridge* definition, it emerges how the pixel number constitute a fundamental parameter that may affect the accuracy of the method. The proposed mathematical algorithm reconstructs the 2D thermal signal with a scaling factor  $R = 2$  by

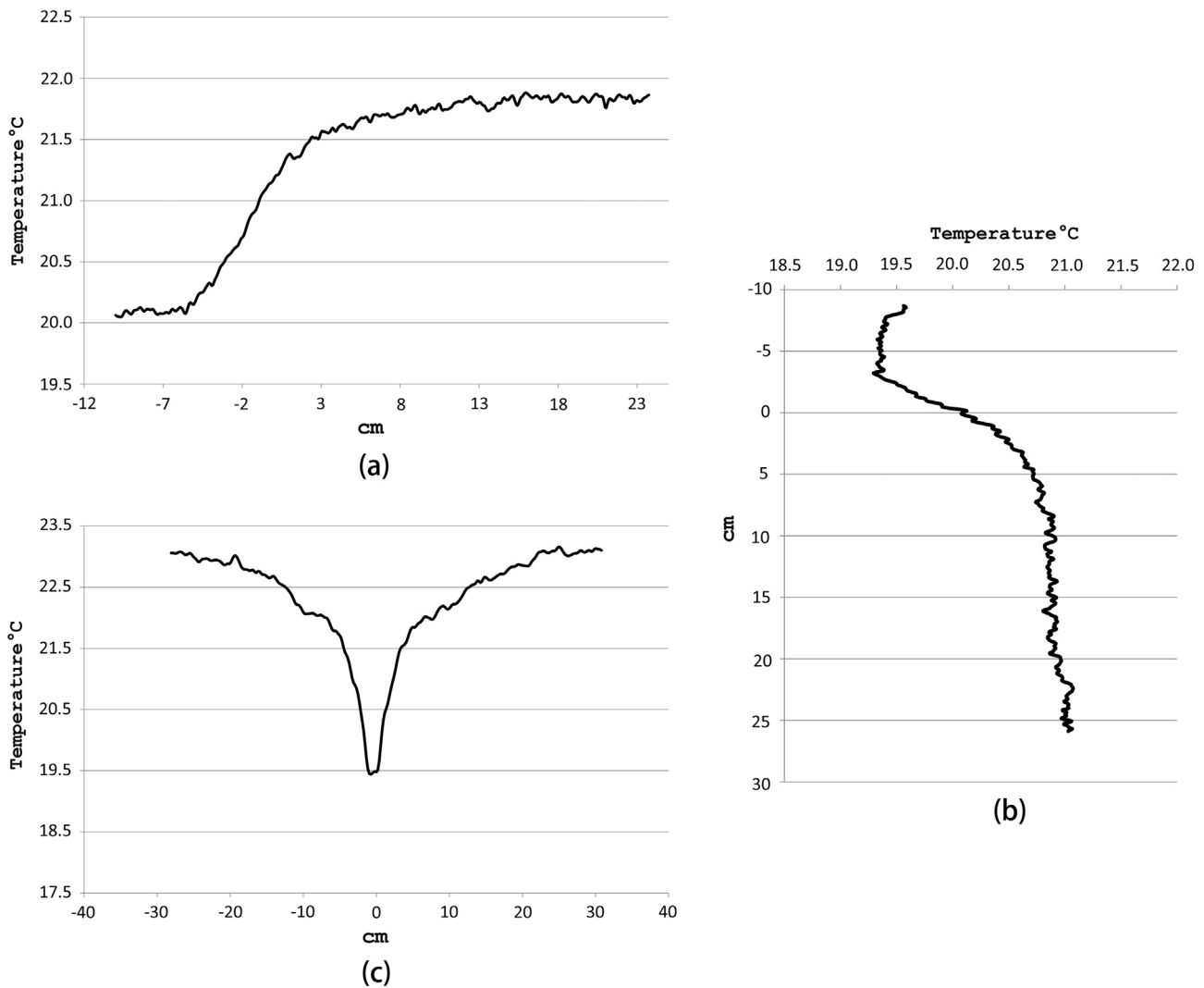


Fig. 10. Temperature trends from the thermograms processed by the proposed mathematical algorithm: TB1 (a), TB2 (b), and TB3 (c).

Table 1

Analysis of the mathematical enhancement effect on the  $I_{tb}$  and  $\psi$  evaluation by infrared thermography on thermal bridges TB1 and TB2.

	Probes	Base method		Enhanced method		Improvement	
	Absolute value	Absolute value	Absolute error	Absolute value	Absolute error	Absolute	Relative
$I_{tb}$ TB1 – pillar	1.439	1.611	+0.172	1.585	+0.146	0.026	1.8%
$I_{tb}$ TB2 – beam-pillar	1.303	1.467	+0.164	1.462	+0.159	0.005	0.4%
$\psi$ TB1 – pillar (W/m/K)	0.05265	0.07328	+0.02063	0.07016	+0.01751	0.00312	5.9%
$\psi$ TB2 – beam-pillar (W/m/K)	0.03849	0.05932	+0.02083	0.05868	+0.02020	0.00064	1.7%

means of a process based on the theory of sampling Kantorovich operators; the choice of  $R = 2$  has been made for technical reasons [18,21,26,27]. The sampling Kantorovich operators application on images processing was validated in previous works on seismic engineering [26,27].

The infrared data have been acquired as an image of resolution of  $320 \times 240$  pixels with an infrared camera (FLIR B360). The mathematical algorithm reconstructs and enhances the image, increasing the resolution up to  $640 \times 480$  pixels. The outcome is a more defined image, and a higher number of pixels to apply the expression of  $I_{tb}$  (Fig. 10).

$I_{tb}$  is connected to the heat losses deriving from thermal bridges through the following equation [17], when the thermal transmittance  $U_{1D}$  of the undisturbed zone is known:

$$\psi = (I_{tb}-1)U_{1D}(l_{tb} + l_{1D}) \tag{3}$$

where  $\psi$  represents the linear thermal transmittance of the thermal bridge itself and  $l_{tb}$  and  $l_{1D}$  stand for the length of the zone affected by the thermal bridge and the length of the undisturbed zone caught by the thermogram, respectively.

The comparative results of the two methods respect to the heat flow meter measurements are reported in Table 1. The new values of the Incidence factor of the thermal bridge for the TB1 and TB2 are closer to the results of the probes methodology, with a sensible deviation for the first thermal bridge and a more little change for the second one. In Table 1 are also reported the absolute and relative improvements due to the mathematical enhancement; the relative improvement is intended as the accuracy increase due to the proposed approach, i.e. the ratio between the absolute improvement and the absolute value obtained by

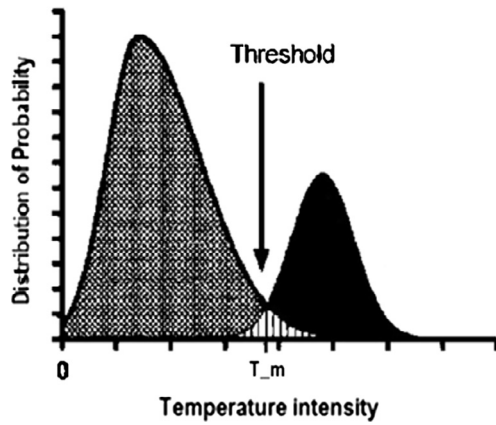


Fig. 11. Generic distribution of probability for the temperature in a thermal bridge.

the sensors.

It emerged that the mathematical algorithm brings to significant improvements, especially on the linear thermal transmittance  $\psi$  estimation, the main parameter characterizing thermal bridges. The sampling Kantorovich operators application on the infrared camera images processing brings to an accuracy enhancement of 5.9% for TB1, validating therefore the method also for thermal applications.

The impact of thermal bridges on the buildings energy loss in different European Member States is considered to walk around 30% [28]. It means that, since the heat loss of a thermal bridge is directly proportional to the linear thermal transmittance  $\psi$ , a measurement more accurate up to about 6% means that the total buildings dispersions could be evaluated with an around 2% higher accuracy with the proposed approach.

Moreover, the results of the algorithm allow a better reading of the structure of thermal bridge: the geometrical boundaries of the different materials that generate the thermal bridge can be extracted defining a threshold parameter, described below, from the analysis of the temperature distribution.

Generally speaking, a thermal bridge is characterized by a significant temperature gradient compared with the average value of the surrounding area (undisturbed zones). The temperature gradient is high when a change of material due to the geometrical contours of thermal bridge structure exists (e.g. contour of a pillar or a beam).

Analysing the histogram associated to the infrared thermal bridge

image, which can be interpreted as the distribution of probability of temperature occurring on the thermal map, two peaks (P1 and P2) representing the homogeneous temperature areas can be identified: one of the undisturbed area of the wall and the other one of the thermal bridge.

Between these two peaks it is possible to find a minimum value which, in view of the above probabilistic interpretation of the data, can be associated to the minimum error due to the wrong classification of pixels located inside the thermal wall but classified as external, and vice versa. The temperature  $T_m$ , which corresponds to the value that minimizes the above misclassification error, identifies the suitable threshold value to segment the thermal bridge shape from the background (Fig. 11).

Fig. 12(a) shows the temperature distribution of the first infrared thermal bridge TB1 with the two peaks (P<sub>1</sub> and P<sub>2</sub>) and the corresponding temperatures ( $T_{p1}$  and  $T_{p2}$ ). For the specific case, the threshold  $T_m$  is equal to 21.3 °C, that is the boundary temperature to create Fig. 12(b), where the red color represents the homogeneous area and the blue zone is the pillar that creates the thermal bridge.

For the TB2 the distribution of temperature and the graphical representation are reported in Fig. 13. In this case, the value of the temperature threshold is equal to 20.1 °C.

Since the sample was built in the laboratory, the accurate geometrical positions of the pillar and the beam can be detected to validate the threshold definition. The difference on TB1 and TB2 between the exact positions of the pillar and the beam and the one obtained by the thermogram analysis were lower than 1 cm in both cases; it has to be noted that the connection among pillar, beam and insulating material was completely covered by the plasterboard, which was the only part of the wall visible to the eye and to the infrared camera. Therefore, it could be stated that the threshold value allows the geometric detection of the different materials constituting the thermal bridge, providing a more precise field of intervention for any correction of the thermal bridge itself.

This methodology finds application only in the types of thermal bridge derived from the presence of different materials inside the wall. Considering the sole geometric nature of the TB3 thermal bridge, the above described procedure has been applied only to TB1 and TB2. It is worth noting that, currently, automatic-non intrusive procedures allowing the detection of the exact boundaries and geometry of thermal bridges do not exist.

Ultimately, the new procedure gives the possibility of realising a thermographic audit on any building envelope, assessing a high

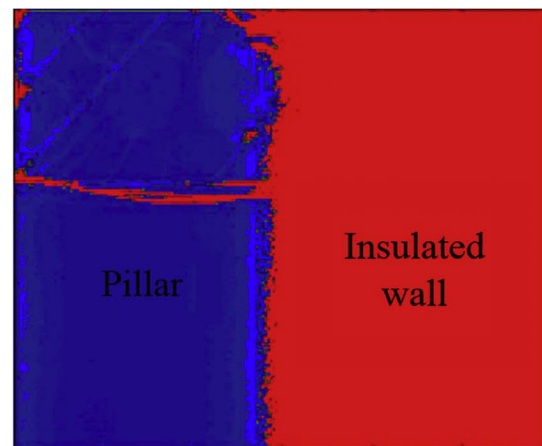
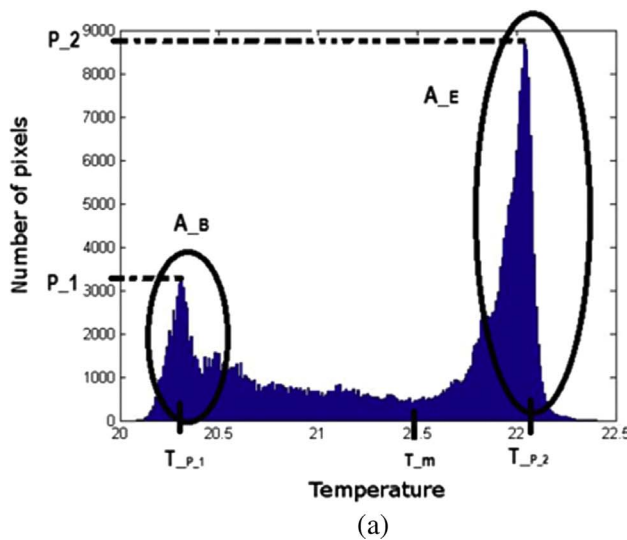


Fig. 12. (a) Distribution of the temperature in the pillar thermal bridge TB1; (b) Boundaries of the structure that generates the thermal bridge retrieved by the distribution of the temperature.

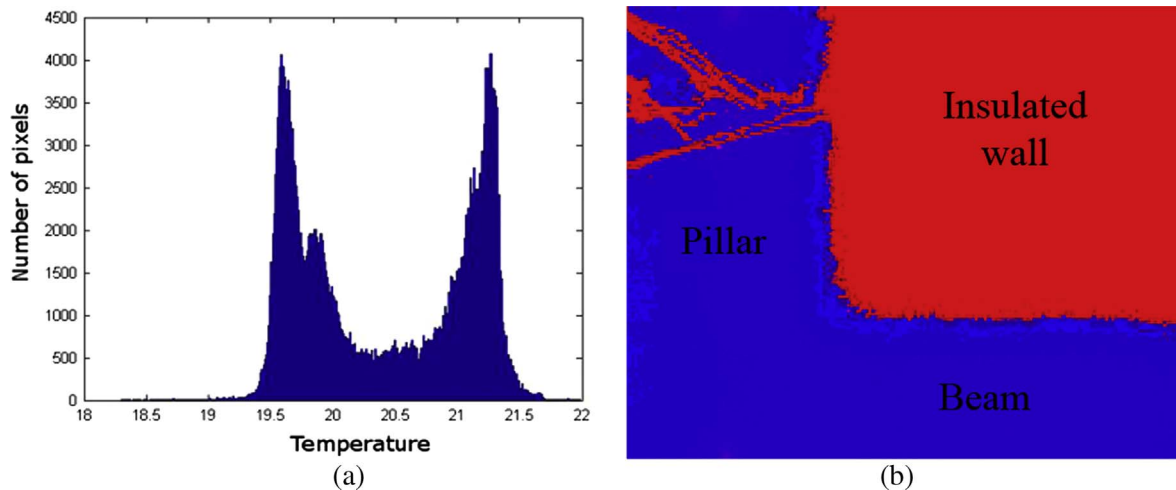


Fig. 13. (a) Distribution of the temperature in the beam corner thermal bridge TB2; (b) Boundaries of the structure that generates the thermal bridge retrieved by the distribution of the temperature.

precision quantification of the thermal bridges with the consequent energy losses, and giving also the information of the different materials boundary of the thermal bridge itself with a completely non-invasive technique, thanks only to a post-processing procedure.

## 6. Conclusions

The infrared thermography is one of the non-destructive methods used to assess the heat transfer in the construction sector. In particular, it is used in the building energy audit to check the anomalies in the opaque and transparent elements causing the thermal bridges.

Although infrared thermography is mainly seen as a qualitative technique, several studies tried to propose indexes or procedures to find suitable values describing the heat transfer. In one of those methodologies [17], the evaluation of the extra-flux passing through a thermal bridge has been proposed, defining an index called *Incidence factor of the thermal bridge* ( $I_{tb}$ ). From the surface temperature measurements, retrieved by the pixels with a correctly framed infrared image, the thermal influence of thermal bridge can be assigned to the corresponding wall where the thermal bridge is positioned.

In order to improve the results of this approach, a mathematical algorithm has been applied to the infrared image to enhance the level resolution and to perform the calculation of the  $I_{tb}$  with a higher precision, so improving the building heat losses evaluation. An experimental campaign has been performed in three types of thermal bridges: (a) pillar; (b) pillar-beam joint; (c) wall-wall joint. Each of them has been built in a hot box apparatus, performing detailed and accurate thermographies, with the acquisition procedure of the image suggested in [17]. The images have been elaborated with the proposed enhancement algorithm and the  $I_{tb}$  has been calculated for both elaborations. Moreover, the Incidence factor of the thermal bridge ( $I_{tb}$ ) was experimentally estimated from the information collected by proper probes measuring thermal fluxes and temperatures placed on the surface of the samples. The latter set-up allows to elaborate an accurate evaluation of  $I_{tb}$  with the use of heat flux meters.

The first outcomes of this analysis have demonstrated that for the thermal bridges TB1 and TB2, the improvement of the infrared methodology with the mathematical algorithm, produced results closer to the experimental factor calculated by the probes. The new approach brought to a significant improvement of the method used to quantitatively assessing the thermal bridges effect on building envelope heat losses. By means of the proposed enhanced mathematical approach, the total building heat losses could be experimentally evaluated with an accuracy improvement of about 2% respect to the simple infrared thermography method. This outcome appears quite relevant if it is also

considered that it is obtained only with a post-processing procedure, without increasing the time and resources spent for experimental measurements.

This analysis has shown the potentiality of the imaging processing applied to the energy evaluation of building thermal losses, describing a procedure that can increase the accuracy of the energy diagnosis using a widespread technique like the infrared thermography. Moreover, the procedure has been shown suitable to detect the position of the boundaries of different materials causing a thermal bridge, by a technique no more operator dependent. This approach results therefore particularly useful for the energy retrofit intervention in existing buildings.

## Acknowledgments

The work has been supported by the research project: “Enhancement algorithms of thermographic images to study the influence of thermal bridges in the energetic analysis of buildings” funded by the “Fondazione Cassa di Risparmio di Perugia”. The authors D. Costarelli, M. Seracini, and G. Vinti, are members of the Dipartimento di Matematica e Informatica of the University of Perugia and of the GNAMPA of INdAM (Istituto Nazionale di Alta Matematica). Moreover, D. Costarelli holds a research grant (Post-Doc) funded by the INdAM, and together with M. Seracini, they are partially supported by the 2016 GNAMPA-INdAM project: “Problemi di regolarità nel calcolo delle variazioni e di approssimazione”.

## References

- [1] Directive 2012/27/EU of the European Parliament and of the Council of 25 October on energy efficiency, efficiency, amending Directives 2009/125/EC and 2010/30/EU and repealing Directives 2004/8/EC and 2006/32/EC.
- [2] Baldinelli G, Bianchi F. Windows thermal resistance: infrared thermography aided comparative analysis among finite volumes simulations and experimental methods. *Appl Energy* 2014;136:250–8.
- [3] Baldinelli G. A methodology for experimental evaluations of low-e barriers thermal properties: field tests and comparison with theoretical models. *Build Environ* 2010;45(4):1016–24.
- [4] Kyliili A, Fokaidis PA, Christou P, Kalogirou SA. Infrared thermography (IRT) applications for building diagnostics: a review. *Appl Energy* 2014;134:531–49.
- [5] Khayatian F, Sarto L, Dall’O G. Building energy retrofit index for policy making and decision support at regional and national scales. *Appl Energy* 2017;206:1062–75.
- [6] Hong T, Piette MA, Chen Y, Lee SH, Taylor-Lange SC, Zhang R, Sun K, Price P. Commercial building energy saver: an energy retrofit analysis toolkit. *Appl Energy* 2015;159:298–309.
- [7] Grinzato E, Vavilov V, Kauppinen T. Quantitative infrared thermography in buildings. *Energy Build* 1998;29:1–9.
- [8] Zalewski L, Lassus S, Rousse D, Boukhalfa K. Experimental and numerical characterization of thermal bridges in prefabricated building walls. *Energy Convers*

- Manage 2010;51:2869–77.
- [9] Fox M, Coley D, Goodhewa s, de Wilde P. Thermography methodologies for detecting energy related building defects. *Renew Sustain Energy Rev* 2014;40:296–310.
- [10] Bianchi F, Pisello AL, Baldinelli G, Asdrubali F. Infrared thermography assessment of thermal bridges in building envelope: experimental validation in a test room setup. *Sustainability* 2014;6(10):7107–20.
- [11] Baldinelli G, Bianchi F, Rotili A, Presciutti A. Transient heat transfer in radiant floors: a comparative analysis between the lumped capacitance method and infrared thermography measurements. *J Imaging* 2016;2(3) 22:1–10.
- [12] Lehmann B, Ghazi Wakili K, Frank Th, Vera Collado B, Tanner Ch. Effects of individual climatic parameters on the infrared thermography of buildings. *Appl Energy* 2013;110:29–43.
- [13] Fokaides PA, Kalogirou SA. Application of infrared thermography for the determination of the overall heat transfer coefficient (U-Value) in building envelopes. *Appl Energy* 2011;88:4358–65.
- [14] Albatici R, Tonelli AM, Chiogna M. A comprehensive experimental approach for the validation of quantitative infrared thermography in the evaluation of building thermal transmittance. *Appl Energy* 2015;141:218–28.
- [15] Ohlsson KEA, Olofsson T. Quantitative infrared thermography imaging of the density of heat flow rate through a building element surface. *Appl Energy* 2014;134:499–505.
- [16] O'Grady M, Lechowska AA, Harte AM. Quantification of heat losses through building envelope thermal bridges influenced by wind velocity using the outdoor infrared thermography technique. *Appl Energy* 2017;208:1038–52.
- [17] Asdrubali F, Baldinelli G, Bianchi F. A quantitative methodology to evaluate thermal bridges in buildings. *Appl Energy* 2012;97:365–73.
- [18] Costarelli D, Vinti G. Approximation by nonlinear multivariate sampling-kantorovich type operators and applications to image processing. *Num Funct Anal Opt* 2013;34(8):819–44.
- [19] Costarelli D, Vinti G. Rate of approximation for multivariate sampling Kantorovich operators on some functions spaces. *J Integral Equations Appl* 2014;26(4):455–81.
- [20] Costarelli D, Vinti G. Degree of approximation for nonlinear multivariate sampling Kantorovich operators on some functions spaces. *Numer Funct Anal Opt* 2015;36(8):964–90.
- [21] Costarelli D, Minotti AM, Vinti G. Approximation of discontinuous signals by sampling Kantorovich series. *J Math Anal Appl* 2017;450(2):1083–103.
- [22] Asdrubali F, Baldinelli G. Thermal transmittance measurements with the hot box method: calibration, experimental procedures, and uncertainty analyses of three different approaches. *Energy Build* 2011;43:1618–26.
- [23] Minkina W, Dudzik S. *Infrared Thermography – errors and uncertainties*. West Sussex, UK: Wiley; 2009.
- [24] FLIR System, Reference manual, Thermacam B360; 2007.
- [25] Hukseflux, User manual HFP01 & HFP03 – v1721; 2016.
- [26] Cluni F, Costarelli D, Minotti AM, Vinti G. Applications of sampling Kantorovich operators to thermographic images for seismic engineering. *J Computat Anal Appl* 2015;19(4):602–17.
- [27] Cluni F, Costarelli D, Minotti AM, Vinti G. Enhancement of thermographic images as tool for structural analysis in earthquake engineering. *NDT E Int* 2015;70:60–72.
- [28] Capozzoli A, Gorrino A, Corrado V. A building thermal bridges sensitivity analysis. *Appl Energy* 2013;107:229–43.